Annals of Biomedical Engineering, Vol. 51, No. 6, June 2023 *(© 2022)* pp. 1284–1295
https://doi.org/10.1007/s10439-022-03131-8

Original Article

A New Phantom that Simulates Electrically a Human Blood Vessel Surrounded by Tissues: Development and Validation Against *In-Vivo* Measurements

SOTIRIS P. EVGENIDIS, ANGELIKI CHONDROU, and THODORIS D. KARAPANTSIOS

Department of Chemical Technology and Industrial Chemistry, School of Chemistry, Aristotle University, University Box 116, 541 24 Thessaloniki, Greece

(Received 14 July 2022; accepted 25 December 2022; published online 4 January 2023)

Associate Editor Stefan M. Duma oversaw the review of this article.

Abstract—This study aims to develop a phantom that simulates the electrical properties of a human blood vessel surrounded by tissues, inside which bubbles can be infused to mimic Decompression Sickness (DCS) conditions. This phantom may be used to calibrate novel electrical methods for bubbles detection in humans and study bubble dynamics during DCS. It may contribute to the limitation of *in-vivo* trials and time/effort saving, while its use can be extended to other biomedical applications. To facilitate the design of the phantom, we perform first *in-vitro* measurements in a flow-loop and *in-vivo* measurements in a swine, in order to detect infused bubbles of a few tenths μm—representing Decompression Sickness conditions—in the test liquid flow and blood flow, respectively, by means of "I-VED" EU patented electrical impedance spectroscopy technique. Results show that the proposed phantom, consisting of a spongy specimen soaked in agar gel in the presence of electrolyte with a hole along it, simulates adequately the electrical properties of a human blood vessel surrounded by tissues. I-VED demonstrates pretty high sensitivity to sense micro-bubbles over the partially conductive vessel walls of the phantom or the isolated animal vein, as well as in the flow-loop: bubbles presence increases electrical impedance and causes intense signal fluctuations around its mean value.

Keywords—Phantom, Decompression sickness, Gas volumetric fraction, Bubbles, Electrical impedance.

INTRODUCTION

In-depth understanding of bubble dynamics in biomedical systems attracts more and more interest the last years. Beyond the direct application of bubble dynamics in Decompression Sickness (DCS), they are also of great significance for sonochemistry, contrast echocardiography and drug-delivery mechanism enhancement through tissue and cell membranes.[23] All the above emphasize the importance of *"bubble science"* in medicine and make it necessary to develop novel diagnostics for bubbles detection and quantification.

This study is focusing mainly on the detection of bubbles due to Decompression Sickness, a clinical syndrome caused by intravascular or extravascular bubbles formation as a result of ambient pressure reduction (decompression). DCS clinical manifestations include joint pain, hypesthesia, generalized fatigue and rash.[17] DCS may occur in scuba divers, pilots and compressed air workers. Moreover, there is a risk during extravehicular activities (EVAs) in current space programs, because astronauts go from a cabin pressure of 14.7 psia (1.0 bar) inside the space shuttle or International Space Station (ISS) to the space suit pressure of 4.3 psia (0.29 bar).[28]

Ultrasound methods have been mostly used so far to detect circulating decompression bubbles. They exploit strong acoustic scattering properties of bubbles due to their surface pulsations and impedance mismatch at the gas–liquid interface.[23] Doppler ultrasound method is the most popular for the detection of bubbles in humans. It can detect bubbles down to 30–

Address correspondence to Sotiris P. Evgenidis, Department of Chemical Technology and Industrial Chemistry, School of Chemistry, Aristotle University, University Box 116, 541 24 Thessaloniki, Greece. Electronic mail: sevgenid@chem.auth.gr

40 μm. Alternative ultrasound methods have been also developed to increase detection sensitivity, including B-mode and M-mode imaging, Second Order Ultrasound Field (SURF) imaging and Dual-Frequency Ultrasound (DFU) method. Although obtained results are often ambiguous, it has been shown that DFU method succeeds to detect bubbles around 10 μm in tissues following decompression.[26] Ultrasound methods are considered the "*gold standard*" for *in-vivo* bubbles detection. However, acquisition and interpretation of ultrasound measurements remain strongly operator dependent. Moreover, ultrasound probes are motion sensitive and large enough to apply underneath diving or space suit. These limitations make ultrasound devices incompatible with a wearable, real-time imaging approach for early detection of bubbles aiming to prevent a forthcoming DCS incident.[12]

Recent advancements on bio-electrical impedance technology domain could be exploited to overcome ultrasound imaging limitations. Bio-impedance methods enable non-invasive and effective monitoring of tissue properties by measuring the ability of the tissue to resist electrical current as a function of frequency.[21] They are currently utilized in diverse medical applications such as monitoring and detection of cellular channels transportation, cancer detection, monitoring of heart diseases and cardiac conditions, estimation of lung functions, monitoring of body fitness and estimation of skin hydration.[13] The concept of bio-impedance analysis is also effective in the analysis of vascular system, including vascular tissues and vascular flow. The interruption of blood flow to the heart tissue that may result in a heart attack, for example, induces an increase of impedance.[21] Similarly, blood flow impedance through an artery is expected to increase in the presence of circulating, non-conductive bubbles. Bio-impedance sensors may become a powerful tool for real-time monitoring of bubbles in humans, since they are simple to operate and already compatible with (inexpensive) wearable approach.[29] Furthermore, the use of electrode pads allows to conduct simultaneously multiple impedance measurements for the detection of bubbles in different body parts of astronauts or scuba divers.

Different *in-vitro* and *in-vivo* experiments are necessary to calibrate and validate any new medical diagnostic before its use in clinical practice. *In-vivo* experiments are complicated, hard to repeat and challenging due to ethical and financial issues. *In-vitro* experiments, on the other hand, are free from ethical issues and enable large cost savings. They can simulate the cardiovascular system by using mechanical hydraulic systems such as pumps, tubes and valves.[1,27] Additionally, tissue phantoms are commonly used to resemble the properties of biological tissues. Phantoms provide repeatable tissue-imitating materials with adjustable mechanical, structural, acoustic, electrical properties in order to test new diagnostics, methods and clinical tools. Depending on the application, certain physical properties must be mimicked within a tissue-imitating geometry. In general, tissue phantoms are made from bio-polymers (e.g. agar, agarose, gelatin, gellan gum) and chemically synthesized polymers (e.g. polyvinyl alcohol, polymerized siloxanes, poly vinyl chlorides).[2,22]

Artificial systems that combine simulation of cardiovascular function with proper tissue phantoms are currently of great interest, since recent technological advancements allow them to reconstruct accurately blood hemodynamics in different tissues under both physiological and pathological conditions. As a result, they can contribute in the development of medical diagnostics and the treatment of severe diseases. On one hand, novel artificial circulatory models enable elaborate programming of pulsating blood flow through fine tuning of blood mimicking fluid flow velocity, pressure and oscillation frequency.[18] On the other hand, 3D printing technology is mature enough to build demanding models, such as abdominal aortic aneurysm before and after stent-graft placement.[19] Abovementioned systems are often accompanied by advanced non-invasive vision-based diagnostic techniques for the detailed analysis of flow dynamics and behavior of flexible tissue models.[20]

This study does not concern an entire artificial system and is focusing solely on a tissue model case. Specifically, it aims to develop a soft and durable phantom that simulates the electrical properties of a human blood vessel surrounded by tissues, inside which bubbles can be infused to mimic Decompression Sickness conditions in the human body. This phantom allows the calibration and validation of novel electrical methods for bubbles detection in humans, as well as in-depth investigation of bubble dynamics during DCS with electrical measurements. As a result, it contributes to the limitation of the necessary *in-vivo* trials and time/effort saving. The use of such a phantom may be extended to other biomedical applications as well, e.g. for the diagnosis of other diseases or the assessment of drug-delivery systems through electrical measurements. In this study, the phantom assists the advancement of an EU patented electrical impedance spectroscopy technique (*EP 3 005 942 A1, 2016*) that has been developed for non-invasive, real-time bubbles detection in humans under the umbrella of the European Space Agency Project "In-Vivo Embolic Detector, I-VED" (Contract No.: 4000101764, 2004–2014). I-VED has been calibrated and validated *in-vitro*, using a benchtop flow-loop that provided well-controlled bubbly flow with liquid velocities, bubble sizes and gas

volumetric concentrations similar to those observed during DCS.[4–6,9,10] Obtained results have shown that I-VED is capable of sensing the presence of micro-bubbles in a liquid flow when conducting measurements with electrodes in direct contact with the bubbly flow inside the flow-loop.[4] The phantom is a useful tool to test I-VED capability on sensing micro-bubbles over its partially conductive walls that mimic electrical properties of real tissues and tune it accordingly in view of the *in-vivo* trials that follow. To facilitate the design of the vessel phantom, we performed first preliminary *in-vitro* measurements in a flow-loop and *in-vivo* measurements in a swine as described below.

MATERIALS AND METHODS

We perform three distinct experiments using I-VED in order to sense bubbles infused in: a) A benchtop flow-loop, b) The blood flow of an experimental animal (swine) and c) The new vessel phantom. I-VED operation and micro-bubbles generation technique, which are common in all experiments, are presented first and followed by the description of each experiment.

I-VED Operation

I-VED performs electrical impedance measurements through a pair of electrodes in electrical contact with the bubbly medium of each experiment. Type and positioning of applied electrodes vary and are specified in the description of each experiment separately. A sinusoidal voltage signal with an amplitude of 2 $V_{p\text{-}p}$ and a frequency of 25 kHz is always applied to excite electrically the two-phase system under study. Preliminary tests showed that, in agreement with previous I-VED *in-vitro* studies,[4,10] this is the optimum frequency value in terms of effective electrodes polarization and capacitance contribution elimination. Electrical signal is recorded by a high-resolution 24-bit data acquisition card (E-MU 1616 m, CREATIVE Professional) with a sampling frequency of 192 kHz. A custom Matlab routine is used for digitally processing and filtering of the acquired signal. The final output of data reduction is an electrical impedance time-series which is transformed to gas volumetric fraction (α) time-series through Maxwell model.[14] More details about I-VED operation can be found in a previous study of the authors,[4] where the electrical technique was analytically described.

Micro-Bubbles Generation Technique

This study requires simple and repeatable production of bubbles of a few tenths μm, as those encountered during DCS.[28] This is accomplished employing the "*two-syringe*" technique that has been developed about 40 years ago for foam-based sclerotherapy in hospitals. This method is an ideal tool for our experiments because it can produce well-controlled foams of tiny bubbles and low liquid content, while bubble size distribution remains unchanged over a wide range of processing conditions (e.g. tubing and fluid velocities).[8] The technique consists of two syringes which are connected via a three-way stopcock (Fig. 1a). Initially, the first syringe contains a pre-defined liquid volume and the second one contains a specific volume of air. The foam is then generated by pushing both liquid and gas repeatedly through the connecting tube. As soon as foam is infused in a liquid medium, bubbles are isolated and start to move due to buoyancy or flow conditions.

The optimum operating conditions that provide a bubble size distribution (BSD), which is narrow enough with a peak up to 50 μm, were defined by preliminary tests. The two-syringe technique was employed for varying number of piston strokes (10—30) and liquid/gas volume ratio (L/G: 1/4–4/1), while the liquid phase consisted of sterile saline (0.9% w/v NaCl, ρ = 1.052 g/ml, μ = 1.01 mPa.s) with the addition of 500 ppm SDS anionic surfactant (Sodium Dodecyl Sulfate, Sigma–Aldrich) that hinders bubbles coalescence. Sterile saline is commonly used in biomedical studies to represent blood,[15] while SDS is also utilized for biological purposes such as in drug carrier systems.[25] Produced foams were infused in a transparent beaker filled with sterile saline, and BSDs of rising bubbles were determined by means of BubbleSEdit software that processed images taken by CANON EOS 350D still digital camera equipped with proper macro lens (CANON EF100mm, f/2.8 Macro USM) and extension rings (CANON, 13–21-31 mm).[31] Obtained BSDs are shown in Figs. 1(b) and 1(c). Although unaffected by the number of piston strokes, they become narrower and sharper with the increase of liquid/gas volume ratio. The combination of L/G: 4/1 with 10 piston strokes seems to fulfil the current needs, since average bubble diameter, D_b, is ~ 30 μm with a standard deviation of ~ 10 μm, and therefore will be applied for well-controlled micro-bubbles production in the three experiments described below.

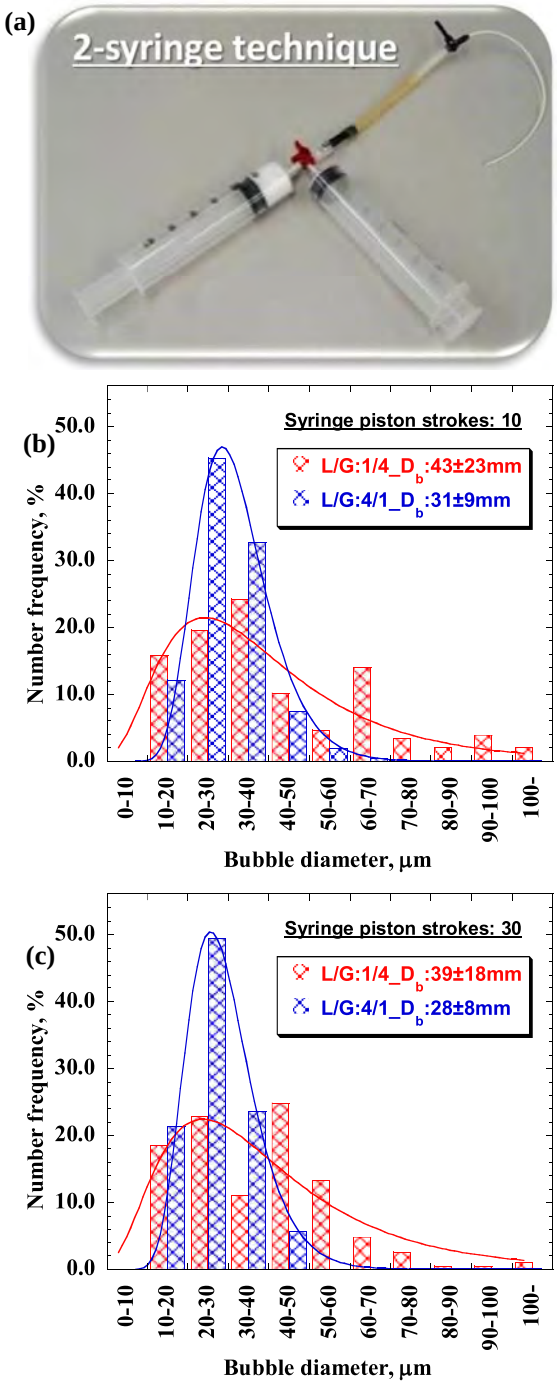

FIGURE 1. (a) Two-syringe technique for micro-bubbles production, (b) bubble size distributions for 10 syringe piston strokes and varying liquid/gas volume ratio, (c) bubble size distributions for 30 syringe piston strokes and varying liquid/gas volume ratio.

Experiment 1: Preliminary In-Vitro Testing in Benchtop Flow-Loop

This experiment conducts I-VED electrical impedance measurements to detect a small amount of bubbles ~ 30 μm, as produced by the abovementioned method, in a benchtop flow-loop. The entire experimental setup is shown in Fig. 2. 500 ml of sterile saline is added in a glass beaker and recirculated through flexible silicon tubes by means of a liquid (aquarium) pump, to represent blood circulation in human vessels. Tube inner diameter, D = 6 mm, is approximating the diameter of swines' jugular vein where *in-vivo* tests are next performed. Liquid flow rate is adjusted to 170 ml/min that corresponds to a superficial velocity, U_{sl}, of 10 cm/s, within the range of blood velocities encountered in the human body. Corresponding Reynolds number of the liquid phase, Re_l, equals to 630 and indicates pure laminar flow conditions. A test section made of PMMA cylindrical tube that accommodates two ring electrodes, flush mounted to its inner walls, is placed at the top of the flow-loop's vertical part to enable electrical and optical measurements of the upward bubbly flow (Fig. 2). The inner diameter of the PMMA tube is 6 mm, while both the width and the separating distance of the ring electrodes are 3 mm (equal to D/2). Micro-bubbles are formed by means of the two-syringe technique as described above and infused in the flowing liquid via a needle, pinned at the bottom of the flow-loop's vertical part. As bubbles rise inside the vertical tube, the bubbly flow passes through the test section where: a) I-VED electrical impedance measurements are conducted through the pair of ring electrodes to sense bubbles presence and b) Bubbly flow images are taken by CANON EOS 350D still digital camera to validate bubble sizes. All in all, the boundary conditions for the analysis in the upward bubbly flow include the following: vertical vessel orientation, D = 6 mm, U_{sl} = 10 cm/s, T = 25 °C, D_b = 30 ± 10 μm.

Experiment 2: Preliminary In-Vivo Testing in Swine

This experiment performs electrical measurements to sense bubbles ~ 30 μm infused in an isolated vein of a swine. Swines are extensively used as biomedical animal models because they are anatomically quite similar to humans and, also, susceptible to common human diseases.[11] Experiment is conducted in the Clinic of Companion Animals of the Faculty of Veterinary Medicine (Aristotle University of Thessaloniki, Greece), with the approval of the Department of Veterinary Medicine (Region of Central Macedonia, Greece), Ref. No 9043/586. A clinically healthy swine of Topics hybrids/Netherlands genetic background at the age of 90 days and body weight of 40 kg is used for this clinical trial. Anaesthesia of the experimental animal is initially induced with propofol (20–50 mg) to affect intravenously until endotracheal intubation can be easily performed and, then, is maintained with isoflurane in oxygen. Cardiovascular and respiratory parameters of the swine

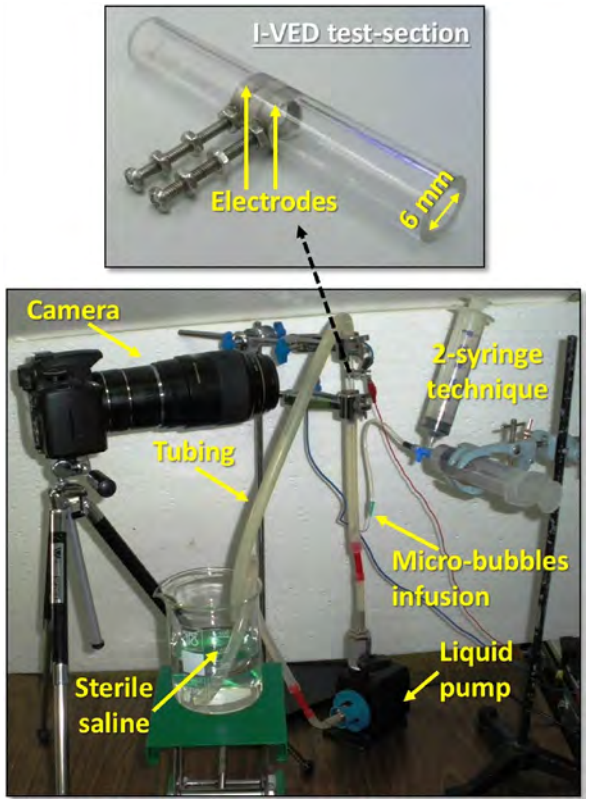

FIGURE 2. Experimental setup for *in-vitro* testing of I-VED capability on sensing a small amount of bubbles ~ 30 μm, as produced by the two-syringe technique, in a benchtop flow-loop.

are monitored during the whole procedure with a Datex-Ohmeda S5 device. Jugular vein is considered the suitable vessel for I-VED testing due to ease of access as concerns the surgical procedure and the appropriate isolation from the surrounding tissues that enables firm placement of I-VED electrodes. Blood flow through jugular vein (D = 6 mm) is laminar, since Re_l equals to 120 (measured blood velocity with Doppler ultrasound ~ 10 cm/s, $\mu \sim 5$ mPa.s at a shear rate of 94 s^{-1}).[30] The procedure of jugular vein isolation and attachment of two plate electrodes (1 cm x 1 cm) on its external walls (one opposite the other) to conduct I-VED measurements for sensing the presence of infused bubbles (~ 30 μm) in the vein, can be shown in Fig. 3. Suppressing of local bleeding is crucial to avoid short-circuits and acquire qualitative electrical signals. I-VED measurements are validated against ultrasound ones performed with T3000 (Terason) ultrasound system equipped with a 6 MHz linear (Hockey stick) array transducer. The boundary conditions for the analysis in the isolated jugular vein include the following: horizontal vessel orientation, D ~ 6 mm, blood velocity ~ 10 cm/s, T = 37 °C, D_b = 30 ± 10 μm.

Experiment 3: Development and Validation of the Vessel Phantom

Here, we describe the preparation and testing of the vessel phantom. The idea is to use a solid material that imitates the electrical properties of human tissues and open a hole through and along this material. The resulting configuration simulates a blood vessel surrounded by tissues. Then, the vessel phantom is filled with the test liquid and I-VED is applied to sense non-intrusively the presence of infused bubbles. The entire experimental setup is depicted in Fig. 4a.

Different polysaccharide-based gels have been used so far to produce electrically conductive phantoms with the addition of conductive nanoparticles or salts and,[3,24] among them, agar gel is the most common one.[15] To combine softness with mechanical stability, the phantom is prepared by a spongy material soaked in agar gel as described below. First, a rectangular spongy specimen of high durability and absorbance (NICOLS Handelsges, mbH, Hamburg) is drilled to open a hole along it with a diameter of 21 mm (Fig. 4b). This is the diameter of human vena cava where bubbles gather during DCS.[27] Next, an aqueous solution of agar (Sigma-Aldrich) 1.5% w/w and NaCl (Merck KGaA) 0.02% w/w is heated to 85 °C at continuous stirring and kept at that temperature for 15 min. Then the spongy specimen is immersed into the viscous solution and squeezed until all air is removed and the liquid fills all its pores. The sponge is removed from the agar solution and left to cool in room temperature to let gel to set. Agar and NaCl concentrations were adjusted to result in a phantom's measured effective electrical conductivity of 1.6–1.7 mS/cm. This corresponds to an electrical resistivity of ~ 600 Ω.cm, which equals to the average value of 21 different human tissues.[7] Finally, the spongy specimen is placed on a specially developed support to minimize liquid leakage and the vessel is filled with sterile saline (14.5 mS/cm or inversely ~ 69 Ω.cm). Micro-bubbles are infused at the bottom of the vessel phantom as shown in Fig. 4a and I-VED measurements for their detection are performed by a pair of plate electrodes 1 cm x 1 cm (Fig. 4c) attached on the external walls of the vessel phantom (thickness: 0.5 cm), one opposite the other (Fig. 4a). The boundary conditions for the analysis in the vessel phantom include the following: vertical vessel orientation, D = 21 mm, T = 25 °C, D_b = 30 ± 10 μm.

Statistical Analysis

Repeatability in gas volumetric fraction measurement is ± 10%. This value corresponds to the coefficient of variation (CV, %) of α, as resulted from

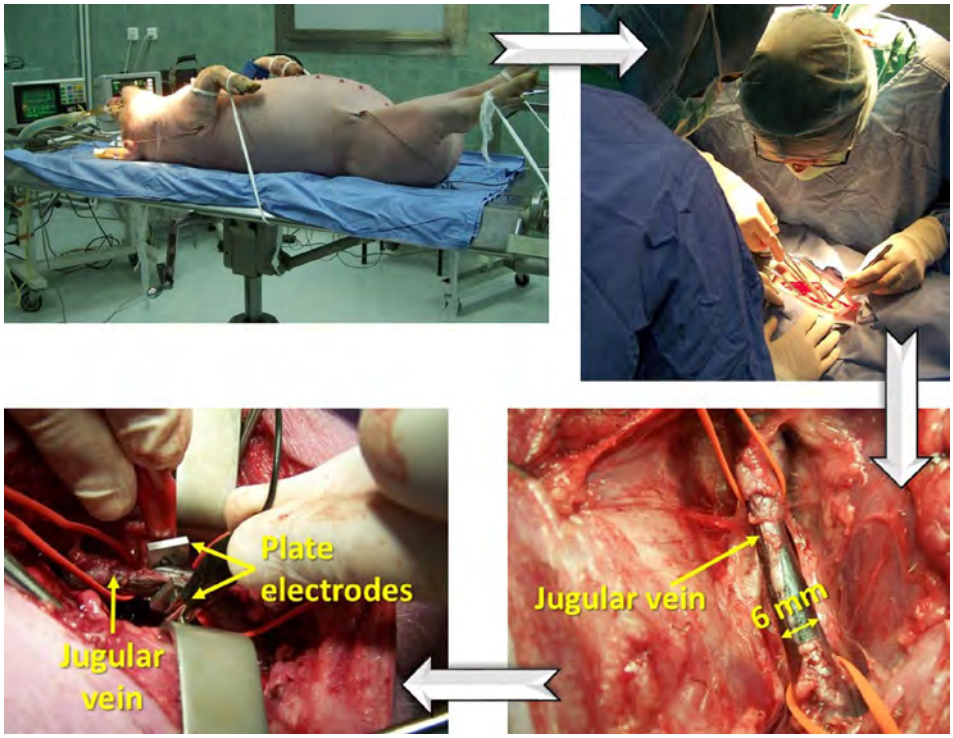

FIGURE 3. The procedure of jugular vein isolation and attachment of two plate electrodes on its external walls (one opposite the other) to conduct I-VED measurements for sensing the presence of infused bubbles (~ 30 μm) in the vein.

successive electrical impedance measurements under the same experimental conditions, and reflects the deviation due to the manual infusion of bubbles in the liquid medium. It is worth noticing that the corresponding CV value of α measured with I-VED technique in bubbly flow with constant gas and liquid flow rates was less than $\pm$ 1%.[4]

RESULTS

Figures 5, 6 and 8 present electrical measurements conducted with I-VED aiming to sense the presence of bubbles 30 $\pm$ 10 μm in a benchtop flow loop (*in-vitro*), in the blood flow of a swine (*in-vivo*) and in the new vessel phantom, respectively. For simplicity, electrical impedance is expressed as electrical resistance since the measured phase of the signals is always close to zero implying pure ohmic behavior of the systems under study. Figure 5a shows the evolution of electrical resistance, R, as a function of time, where R value shows insignificant variation for the first 5 s due to the absence of bubbles in the flow-loop (single-phase/liquid flow, baseline measurement). The time-point of bubbles infusion in the flow-loop is denoted with the red line in Fig. 5a. As soon as rising bubbles reach I-VED electrodes, R starts to increase (blue line) because air is more resistive than the sterile saline flowing in the flow-loop. The average value of R increases gradually for 7–8 s and remains almost constant for ~ 8 s, before to start decreasing as the amount of infused bubbles gets lower. Bubbles presence disturbs the electric field between the electrodes and, as a result, increases the intensity of I-VED signal fluctuations from 5 to 25 s. Electrical resistance time-series after the time-point of bubbles detection (Fig. 5a) is transformed to gas volumetric fraction (α) time-series employing Maxwell model,[14] Fig. 5b. The trend of gas volumetric fraction signal is similar with that of electrical resistance signal, while the maximum value of α is around 1.5% that is not considered too high for a DCS incident.

Figure 6a shows the electrical resistance time-series for I-VED *in-vivo* testing, where red and blue lines indicate the time-points of bubbles infusion and sensing in the jugular vein of the swine, respectively. As expected, baseline electrical signal (before bubbles infusion) is not as steady as in Fig. 5a. However, the presence of micro-bubbles, validated by the ultrasound measurements as shown in Fig. 7, clearly increases both the average value of R and the intensity of signal fluctuations. Figure 6b presents the estimated gas volumetric fraction, α, inside the jugular vein as a function of time, after the time-point of bubbles detection. Although α reaches temporarily a maximum value of ~ 3%, it varies mostly between 0.5% and 2%

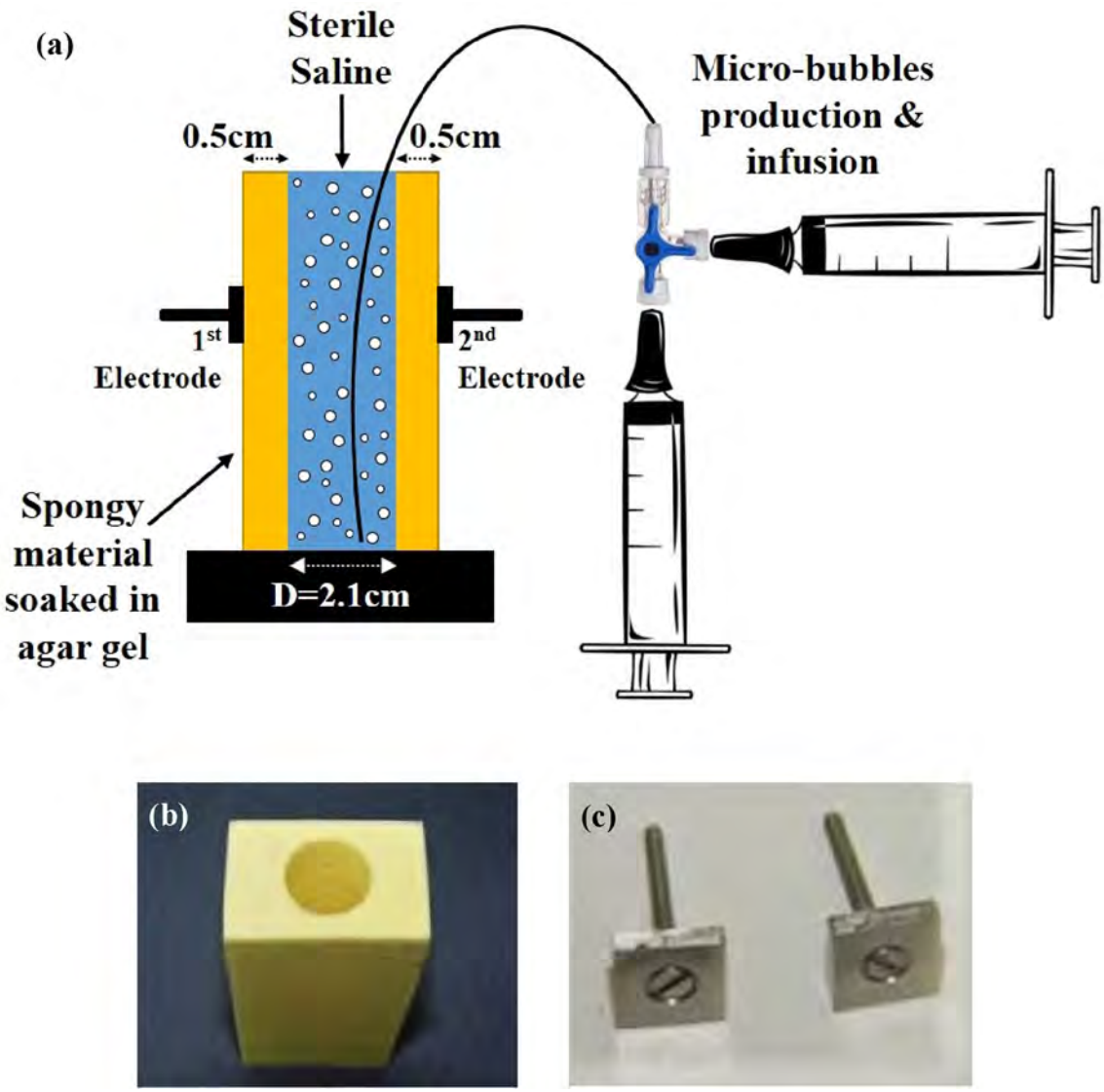

FIGURE 4. (a) Entire experimental setup for the validation of phantom functionality, (b) Vessel phantom prepared by a drilled spongy material soaked in agar gel, (c) Pair of plate electrodes 1 cm × 1 cm for I-VED measurements on the phantom.

before to start decreasing due to the reduction of bubbles population.

Figure 8 presents I-VED electrical impedance measurements in the vessel phantom, as conducted by a pair of electrodes over its partially conductive walls. A couple of seconds after the addition of sterile saline in the vessel phantom, I-VED performs the baseline measurement for 50 s, i.e. in the absence of micro-bubbles. Figure 8a shows the evolution of electrical resistance, R, as a function of time for this case. It is demonstrated that R decreases constantly with time (black curve in Fig. 8a). Sterile saline is about ten times less resistive than the phantom walls (~ 69 Ω.cm vs ~ 600 Ω.cm) and as the liquid diffuses through the pores of the spongy material, the measured electrical resistance decreases accordingly. To get rid of the diffusion effect, I-VED signal is de-trended following a 3-steps procedure: (a) Identification of the equation that fits adequately the data (a 2nd order polynomial equation in this case), (b) Calculation of predicted R values employing the polynomial equation for the total duration of the time-series, and (c) Subtraction of the predicted R values from original R values to remove the trend. The resulting de-trended electrical resistance time-series is shown in Fig. 8a as well (blue curve). As expected, electrical resistance remains roughly constant in the absence of micro-bubbles (baseline measurement). Preliminary baseline measurements showed that

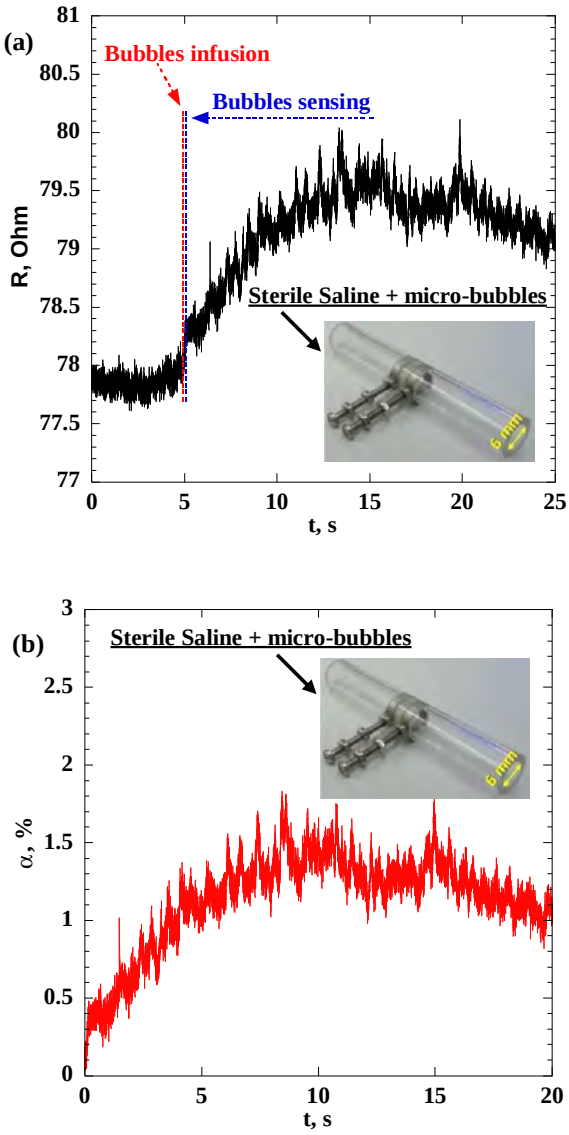

FIGURE 5. Evolution of (a) measured electrical resistance, R, and (b) gas volumetric fraction, α, as a function of time, t, when bubbles 30 ± 10 μm are infused in sterile saline that recirculates in the benchtop flow-loop.

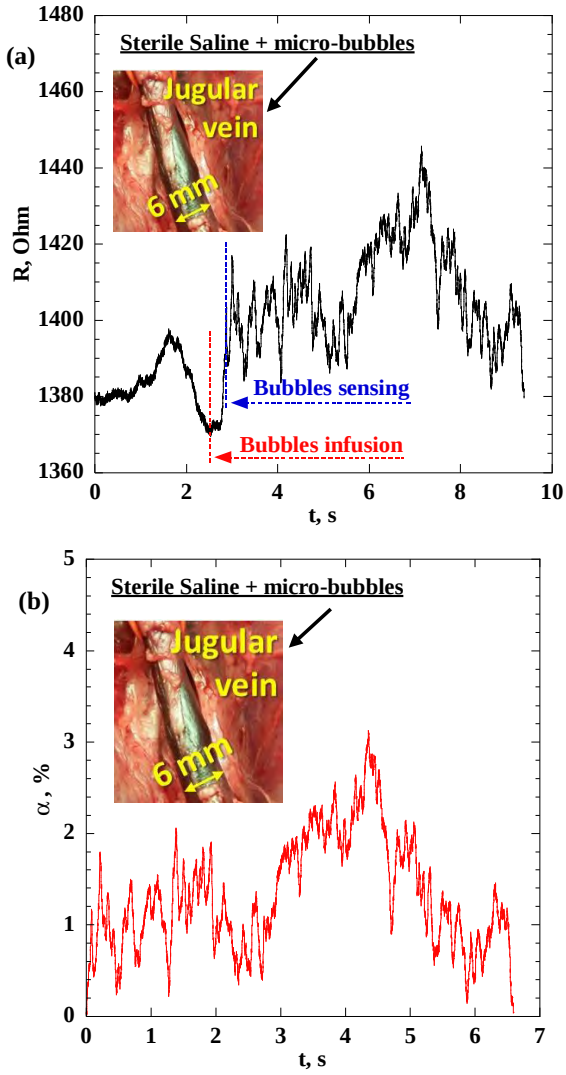

FIGURE 6. Evolution of (a) measured electrical resistance, R, and (b) gas volumetric fraction, α, as a function of time, t, when bubbles 30 ± 10 μm are infused in the jugular vein of a swine.

fitting equation remains practically unchanged at least for 3 min. Based on that, the entire experiment lasts approximately 1.5 min to exclude any effect of time (due to the diffusion of saline solution through the spongy material) on de-trending procedure.

Micro-bubbles production by means of the "two-syringe" technique and their infusion at the bottom of the vessel phantom takes place a few seconds after the completion of the baseline measurement, to avoid extensive diffusion of sterile saline through the pores of the spongy material. Figure 8b shows the evolution of R as a function of time during the infusion of bubbles around 30 μm. Similarly to the baseline measurement (black curve in Fig. 8a), electrical resistance decreases with time, the rate of R reduction however is lower due to the addition of highly resistive air bubbles (black curve in Fig. 8b). In addition, rising bubbles in the vessel phantom cause distinct signal fluctuations. When de-trending the raw electrical signal employing the 2nd order polynomial equation defined above, R is affected solely by the bubbles presence and, therefore, increases progressively (blue curve in Fig. 8b). De-trended R time-series is transformed to gas volumetric fraction, α, time-series employing Maxwell model,[14] as shown in Fig. 8c. It is shown that α increases progressively due to bubbles gathering at the top of the phantom, while intense α fluctuations are attributed to bubble swarms that cross electrodes area.

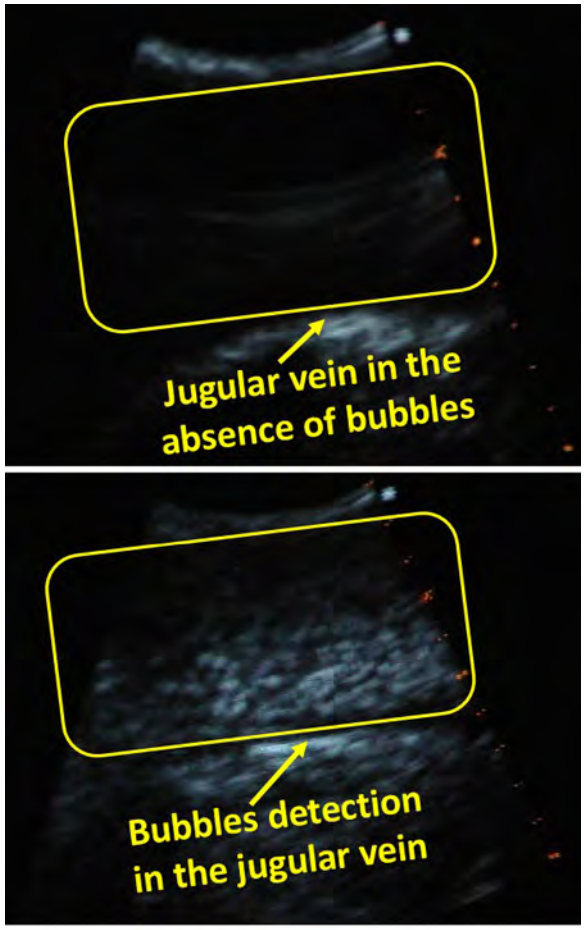

FIGURE 7. Detection of bubbles 30 ± 10 μm inside the jugular vein by means of ultrasound measurements.

DISCUSSION

This work deals with the development of a phantom that simulates the electrical properties of a human blood vessel surrounded by tissues, inside which bubbles are infused to represent DCS conditions. This phantom enables the calibration of new electrical techniques for bubbles detection in humans and the study of bubbly flow features during DCS with electrical measurements. Thus, it limits the necessity for numerous *in-vivo* trials, while its use may be extended to other biomedical applications. Here, the phantom contributes to the advancement of a novel electrical impedance spectroscopy technique, I-VED, for non-invasive, real-time bubbles detection in humans.

First, we determine the optimum conditions for the production of the desired bubbles to be infused in the phantom in order to simulate DCS conditions, by means of the two-syringe technique. When applying a liquid/gas volume ratio of 4/1, where liquid consists of sterile saline with the addition of 500 ppm SDS, in conjunction with 10 piston strokes, bubble sizes range

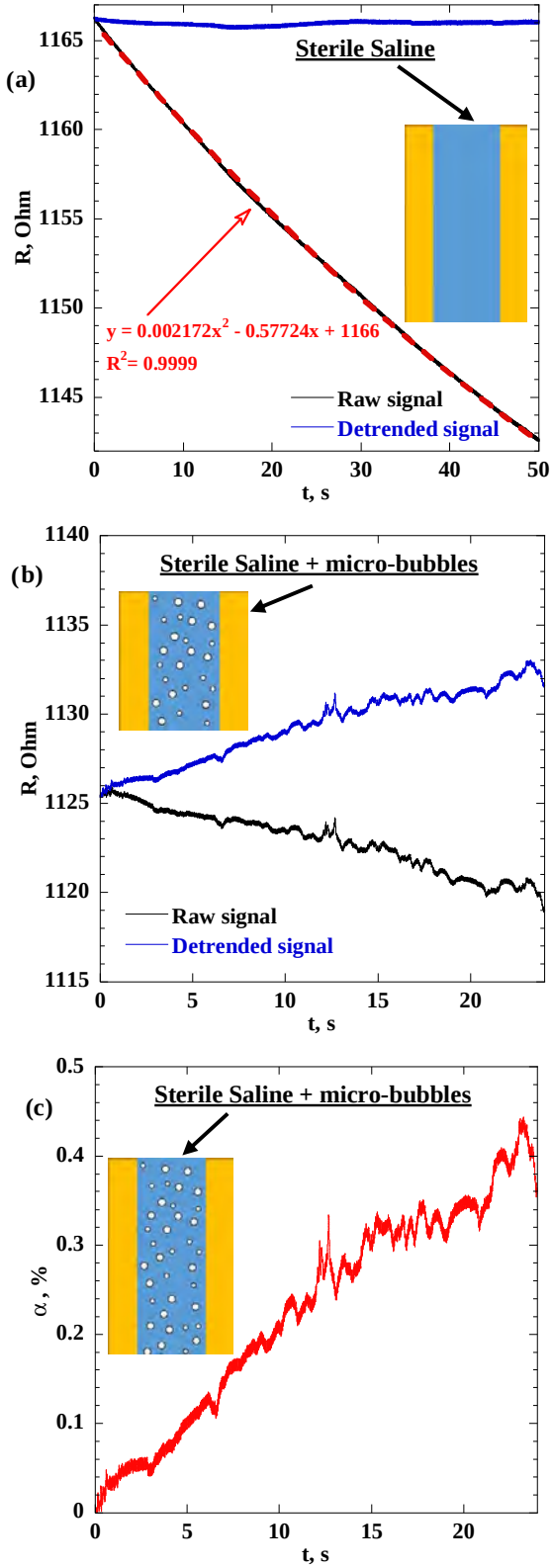

FIGURE 8. Time evolution of (a) electrical resistance when vessel phantom is filled with sterile saline, (b) electrical resistance during bubbles 30 ± 10 μm infusion in the vessel phantom and (c) gas volumetric fraction during bubbles 30 ± 10 μm infusion in the vessel phantom.

from 20 μm to 40 μm. These bubble sizes are commonly encountered in DCS incidents.[28] However, I-VED performance has not been tested so far for such small bubbles. Before employing it in the phantom where electrical measurements are conducted over partially conductive walls, we examine its capability to detect bubbles 30 ± 10 μm in a conventional flow-loop. Bubbles detection is less complicated in this case, since I-VED electrodes are in direct contact with the bubbly flow. Although bubbles are too small, their presence not only changes the average value of measured signal, but also causes clear fluctuations around it and this is a strong evidence of high I-VED measuring sensitivity. This behavior is also noticed in: (a) previous similar studies of the authors, concerning gas–liquid flows of varying gas volumetric fractions, gas/liquid phase velocities, liquid phase properties, bubble sizes and pipe diameters,[4,9,10,16] and (b) other two-phase flow applications, such as oil–water two-phase flows encountered in petroleum and chemical industries and gas–liquid slug flows in mini-channels found e.g. in heat exchangers and biochemical analysis devices. In any case, the intensity and the frequency of electrical impedance signal fluctuations strongly depend on the size and quantity of particles (bubbles or droplets).[32,33]

Next, it was considered essential to perform an *in-vivo* trial in an effort to facilitate the design of the phantom and validate its functionality. Thus, bubbles of 30 ± 10 μm are infused in the jugular vein of a swine and I-VED measurements are conducted by a pair of plate electrodes attached on the external walls of the vessel in order to: a) Demonstrate whether I-VED can sense bubbles when electrodes are not in direct contact with the bubbly medium, b) Provide a useful range of measured impedance values. Although electrical measurements are performed over partially conductive vessel walls that result in much higher R values (1400 ± 50 Ohm) compared to the previous experiment (~ 80 Ohm), I-VED is shown again sensitive enough to sense bubbles presence. The micro-bubbles increase measured electrical resistance and signal amplitude as well. Based on that, acquired *in-vivo* signals share common qualitative features with *in-vitro* ones for varying vessel diameters, α values, gas and phase velocities and properties, as well as dispersed phase nature (gas bubbles or liquid droplets).[4,9,10,16,32,33] It is interesting to notice that estimated gas volumetric fraction in jugular vein (D = 6 mm) is quite close to that in the flow-loop (D = 6 mm), despite the differences in measured R values and contact of electrodes with the bubbly medium.

After the completion of the preliminary tests, the vessel phantom is produced by a spongy material soaked in agar gel in the presence of electrolyte, through which a hole of 21 mm is opened to represent vena cava surrounded by tissues. The concentration of the electrolyte is properly adjusted to result in a phantom's electrical resistivity value, ~ 600 Ω.cm, which is equal to the mean value of 21 different human tissues.[7] This value is used to simulate the forthcoming *in-vivo* tests on humans, where I-VED electrodes will be attached on the skin to sense the presence of bubbles in the bloodstream over a medium composed by different tissue layers (e.g. muscle, fat and skin). The phantom is filled with sterile saline and micro-bubbles are infused at its bottom to simulate DCS conditions. In parallel, I-VED performs electrical measurements with two plate electrodes attached on the external walls of the phantom. Measured electrical resistance ranges from 1100 to 1200 Ohm, which is not far from R values measured in the jugular vein of the swine (1400 ± 50 Ohm). In both cases, electrical measurements are conducted over partially conductive walls and noticed closeness of R values indicates that phantom simulates fairly electrical properties of real tissues. Although wall thickness of the phantom is larger than this of the jugular vein aiming to mimic successive tissue layers, I-VED is still capable of detecting micro-bubbles presence since recorded R value and signal amplitude clearly increase. By a qualitative point of view, no noteworthy difference is noticed in signal characteristics comparing to abovementioned *in-vitro* and *in-vivo* experiments.[4,9,10,16,32,33] As expected, measured gas volumetric fraction in the phantom is lower comparing to this measured in the jugular vein, since micro-bubbles are infused in a vessel of much larger diameter, 21 mm vs 6 mm. In a future study, it would be interesting to investigate whether the fluctuations of such gas volumetric fraction signals could be used to determine average bubble size, as already done for the case that electrodes are in direct contact with the bubbly flow.[4,9,10]

Limitations of the Study

Limitations of this study are listed below:

- Although simple enough, manual production and infusion of bubbles makes it difficult to obtain steady as well as repeatable bubbly flow conditions in all experiments conducted in this study. As a result, in contrast with our previous studies where constant gas and liquid flow rates ensured pretty steady two-phase flow conditions,[4,9,10,16] non-negligible instability can be clearly noticed in acquired electrical impedance signals (Figs. 5, 6). Additionally, limited repeatability in micro-bubbles infusion

(unsteadiness of manual infusion and bubbles velocity) deteriorates considerably the repeatability in gas volumetric fraction measurement under the same experimental conditions.

- Even if bubbles detection by means of I-VED technique is evident in all experiments due to both electrical resistance and signal amplitude increase, the measurement of gas volumetric fraction is not validated with another established method. However, it is worth noticing that its calculation is based on a well-established method applied extensively in literature.[4,9,10,16]
- The objective of I-VED measurement on isolated jugular vein was dual: a) To test I-VED capability on detecting bubbles over partially conductive vein walls, and b) Provide a useful range of measured impedance values. Although the present work is mostly a proof of concept study as concerns phantom and I-VED performance, a number of I-VED measurements on veins surrounded by tissues could be beneficial for phantom validation and I-VED development as a non-invasive tool for early detection and quantification of bubbles. However, it requires systematic work and significant effort and is beyond the scope of this study.

Future studies shall improve the procedure of micro-bubbles production and infusion, include gas volumetric fraction validation and examine *in-vivo* bubbles detection capability of I-VED over a layer of tissues with varying depth and complexity.

CONCLUSIONS

The proposed vessel phantom, consisting of a spongy material soaked in agar gel in the presence of electrolyte through which a hole of the desired diameter (corresponding to a specific vein) is opened, is shown to simulate adequately the electrical properties of a human blood vessel surrounded by tissues. As a result, it allows the detection of infused bubbles inside its hole—representing Decompression Sickness conditions—by means of electrical measurements. The functional validation of the vessel phantom is performed with "I-VED" EU patented electrical impedance spectroscopy technique. I-VED demonstrates pretty high sensitivity to detect bubbles of a few tenths μm without direct contact of electrodes and bubbly medium, over partially conductive vessel walls, either in the phantom or in an isolated animal vein. To the best of our knowledge, this is the first time that an electrical technique accomplishes such a task and, therefore, I-VED needs to be thoroughly tested both *in-vitro* (using the new phantom) and *in-vivo* in order to examine its effectiveness on non-invasive detection of bubbles in humans and evaluate the detection limits.

ACKNOWLEDGMENTS

Authors are really thankful to Prof. L. Papazoglou, Prof. I. Savvas, Prof. M. Patsikas and Dr. K. Pavlidou from the Faculty of Veterinary Medicine (Aristotle University of Thessaloniki, Greece) for their contribution in organizing and performing *in-vivo* trial. This study was funded by GSTP Project: In-Vivo Embolic Detector, I-VED-Contract No.: 4000101764. The view expressed herein can in no way be taken to reflect the official opinion of the European Space Agency.

CONFLICT OF INTEREST

All authors certify that they have no affiliations with or involvement in any organization or entity with any financial interest or non-financial interest in the subject matter or materials discussed in this manuscript.

REFERENCES

[1]Adams, F., T. Qiu, A. Mark, B. Fritz, L. Kramer, D. Schlager, U. Wetterauer, A. Miernik, and P. Fischer. Soft 3D-printed phantom of the human kidney with collecting system. *Ann. Biomed. Eng*. 45:963–972, 2017.

[2]Anand, G., A. Lowe, and A. Al-Jumaily. Tissue phantoms to mimic the dielectric properties of human forearm section for multi-frequency bioimpedance analysis at low frequencies. *Mat. Sci. Eng. C*. 96:496–508, 2019.

[3]Brzozowski, P., K. I. Penev, and K. Mequanint. Gellan gum gel tissue phantoms and gel dosimeters with tunable electrical, mechanical and dosimetric properties. *Int. J. Biol. Macromol*. 180:332–338, 2021.

[4]Evgenidis, S., and T. Karapantsios. Effect of bubble size on void fraction fluctuations in dispersed bubble flows. *Int. J. Multiph. Flow*. 75:163–173, 2015.

[5]Evgenidis, S., and T. Karapantsios. Gas–liquid flow of submillimeter bubbles at low void fractions: experimental study of bubble size distribution and void fraction. *Int. J. Heat Fluid Fl*. 71:353–365, 2018.

[6]Evgenidis, S. P., and T. D. Karapantsios. Gas–liquid flow of sub-millimeter bubbles at low void fractions: Void fraction prediction using drift-flux model. *Exp. Therm. Fluid. Sci*. 98:195–205, 2018.

[7]Faes, T. J. C., H. A. van der Meij, J. C. de Munck, and R. M. Heethaar. The electric resistivity of human tissues (100 Hz–10 MHz): a meta-analysis of review studies. *Physiol. Meas*. 20:R1, 1999.

[8]Gaillard, T., M. Roche, C. Honorez, M. Jumeau, A. Balan, C. Jedrzejszyk, and W. Drenckhan. Controlled foam generation using cyclic diphasic flows through a constriction. *Int. J. Multiphas. Flow*. 96:173–187, 2017.

[9]Gkotsis, P., S. P. Evgenidis, and T. D. Karapantsios. Associating void fraction signals with bubble clusters features in co-current, upward gas-liquid flow of a non-Newtonian liquid. *Int. J. Multiphas. Flow*. 131:103297, 2020.
[10]Gkotsis, P., S. P. Evgenidis, and T. D. Karapantsios. Influence of Newtonian and non-Newtonian fluid behaviour on void fraction and bubble size for a gas-liquid flow of sub-millimeter bubbles at low void fractions. *Exp. Therm. Fluid. Sci*. 109:109912, 2019.
[11]Kaser, T. Swine as biomedical animal model for T-cell research—Success and potential for transmittable and non-transmittable human diseases. *Mol. Immunol*. 135:95–115, 2021.
[12]Le, D. Q., P. A. Dayton, F. Tillmans, J. Freiberger, R. Moon, P. Denoble, and V. Papadopoulou. Ultrasound in decompression research: fundamentals, considerations, and future technologies. *Undersea Hyperb. Med*. 48(1):59–72, 2021.
[13]Li, Y., R. Ma, X. Wang, J. Jin, H. Wang, Z. Liu, and T. Yin. Tissue coefficient of bioimpedance spectrometry as an index to discriminate different tissues in vivo. *Biocybern. Biomed. Eng*. 39(3):923–936, 2019.
[14]Maxwell, J. C. A Treatise of Electricity and Magnetism. London: Oxford University Press, 1892.
[15]Nebuya, S., M. Noshiro, B. H. Brown, R. H. Smallwood, and P. Milnes. Detection of emboli in vessels using electrical impedance measurements—phantom and electrodes. *Physiol. Meas*. 26:111–118, 2005.
[16]Oikonomidou, O., S. P. Evgenidis, M. Kostoglou, and T. D. Karapantsios. Degassing of a pressurized liquid saturated with dissolved gas when injected to a low pressure liquid pool. *Exp. Therm. Fluid Sci*. 96:347–357, 2018.
[17]Papadopoulou, V., S. Evgenidis, R. J. Eckersley, T. Mesimeris, C. Balestra, M. Kostoglou, T. D. Karapantsios, and M. X. Tang. Decompression induced bubble dynamics on ex vivo fat and muscle tissue surfaces with a new experimental set up. *Colloids Surf. B*. 129:121–129, 2015.
[18]Polanczyk, A., M. Klinger, J. Nanobachvili, I. Huk, and C. Neumayer. Artificial circulatory model for analysis of human and artificial vessels. *Appl. Sci*. 8:1017, 2018.
[19]Polanczyk, A., M. Podgorski, M. Polanczyk, A. Piechota-Polanczyk, C. Neumayer, and L. Stefanczyk. A novel patient-specific human cardiovascular system phantom (HCSP) for reconstructions of pulsatile blood hemodynamic inside abdominal aortic aneurysm. *IEEE Access*. 6:61896–61903, 2018.
[20]Polanczyk, A., M. Podgorski, M. Polanczyk, A. Piechota-Polanczyk, L. Stefanczyk, and M. Strzelecki. A novel vision-based system for quantitative analysis of abdominal aortic aneurysm deformation. *Biomed. Eng. OnLine*. 18:56, 2019.
[21]Prasad, A., and M. Roy. Bioimpedance analysis of vascular tissue and fluid flow in human and plant body: a review. *Biosyst. Eng*. 197:170–187, 2020.
[22]Rajeshkumar, G., R. Vishnupriyan, and S. Selvadeepak. Tissue mimicking material an idealized tissue model for clinical applications: a review. *Mater. Today*. 22:2696–2703, 2020.
[23]Rivera, M., E. Lopez, and S. Cancelos. A non-invasive, low frequency resonant method to detect bubbles in liquid media. *Appl. Acoust*. 179:108044, 2021.
[24]Serafin, A., C. Murphy, M. C. Rubio, and M. N. Collins. Printable alginate/gelatin hydrogel reinforced with carbon nanofibers as electrically conductive scaffolds for tissue engineering. *Mater. Sci. Eng. C*. 122:111927, 2021.
[25]Sharma, G., M. Naushad, B. Thakur, A. Kumar, P. Negi, R. Saini, A. Chahai, F. J. Stadler, and U. M. H. Aqil. Sodium dodecyl sulphate-supported nanocomposite as drug carrier system for controlled delivery of ondansetron. *Int. J. Environ. Res. Public Health*. 15:414, 2018.
[26]Swan, J. G., J. C. Wilbur, K. L. Moodie, S. A. Kane, D. A. Knaus, D. Phillips, T. L. Beach, A. M. Fellows, P. J. Magari, and J. C. Buckey. Microbubbles are detected prior to larger bubbles following decompression. *J. Appl. Physiol*. 116:790–796, 2014.
[27]Tan, X., D. Li, M. Jeong, T. Yu, Z. Ma, S. Afat, K.-E. Grund, and T. Qiu. Soft liver phantom with a hollow biliary system. *Ann. Biomed. Eng*. 49(9):2139–2149, 2021.
[28]Vann, R. D., F. K. Butler, J. Mitchell, and R. E. Moon. Decompression illness. *Lancet*. 377:153–164, 2011.
[29]Vine, S. M., P. L. Painter, M. A. Kuskowski, and C. P. Earthman. Bioimpedance spectroscopy for the estimation of fat-free mass in end-stage renal disease. *E. Spen. Eur. E-J. Clin. Nutr. Metab*. 6:e1–e6, 2011.
[30]Windberger, U., A. Bartholovitsch, R. Plasenzotti, K. J. Korak, and G. Heinze. Whole blood viscosity, plasma viscosity and erythrocyte aggregation in nine mammalian species: reference values and comparison of data. *Exp. Physiol*. 88(3):431–440, 2003.
[31]Zabulis, X., M. Papara, A. Chatziargyriou, and T. D. Karapantsios. Detection of densely dispersed spherical bubbles in digital images based on a template matching technique: application to wet foams. *Colloids Surf. A*. 309:96–106, 2007.
[32]Zhai, L. S., H. M. Wang, C. Yan, H. X. Zhang, and N. D. Jin. Development of empirical correlation to predict droplet size of oil-in-water flows using a multi-scale Poincaré plot. *Exp. Therm. Fluid. Sci*. 98:290–302, 2018.
[33]Zuang, J., Y. Jinag, H. Ji, B. Wang, and Z. Huang. Electrical impedance characteristics of slug flow in small channels and its application to void fraction estimation. *Int. J. Multiphas. Flow*. 156:104200, 2022.